Design of Temporal Basis Functions for Time Domain Integral Equation Methods With Predefined Accuracy and Smoothness

Elwin van 't Wout, Duncan R. van der Heul, Harmen van der Ven, and Cornelis Vuik

***Abstract*—A key parameter in the design of integral equation methods for transient electromagnetic scattering is the definition of temporal basis functions. The choice of temporal basis functions has a profound impact on the efficiency and accuracy of the numerical scheme. This paper presents a framework for the design of temporal basis functions with predefined accuracy and varying smoothness properties. The well-known shifted Lagrange basis functions naturally fit in this framework. New spline basis functions will be derived that have the same interpolation accuracy as shifted Lagrange basis functions and with the added advantage of being smooth. Numerical experiments show the positive influence of smoothness on the quadrature error in the numerical integration procedure. The global accuracy in time of the numerical scheme based on shifted Lagrange and spline basis functions has been experimentally analyzed. For a given interpolation error the experiments confirm the expected accuracy for the shifted Lagrange basis functions, but remarkably show a higher order of accuracy for the spline basis functions.**

***Index Terms*—Computational accuracy, electric field integral equation, interpolation, time domain analysis.**

I. Introduction

TIME DOMAIN integral equation (TDIE) methods can model transient electromagnetic scattering phenomena accurately and efficiently. They are appealing tools for the computational electromagnetic community since the radiation condition is automatically imposed and only the surface of an object has to be discretized. Because the equations are fully formulated in time-domain, the method has the potential to analyze wide-band and nonlinear scattering. Most TDIE methods can function on unstructured triangular meshes and without constraints on the Courant-Friedrichs-Lewy (CFL) number which allows a great flexibility in the choice of spatial and temporal mesh sizes. However, widespread use of TDIE methods has been lagging behind because of instabilities and relatively long computation times. With the inception of accelerators based on plane-wave and fast Fourier techniques the efficiency has been improved such that objects of industrial interest can be modeled [1], [2]. Stability has been enhanced by the combined use of filtering [3], implicit time stepping [4], accurate evaluation of the system matrix [5], carefully tailored temporal basis functions [6], Calderón preconditioning [7], space-time Galerkin discretization [8], and convolution quadrature [9]. Since stable results can be obtained for a very wide range of time step sizes [5], modern TDIE methods can be used for all practical purposes [4].

The marching-on-in-time (MOT) scheme has been used extensively to discretize the electric field integral equation (EFIE). Its marching procedure results in an efficient algorithm. One of the main choices to be made for the MOT scheme is the definition of temporal basis functions. Without any counterpart in frequency domain solvers, many different temporal basis functions have been proposed in the literature [6], [10]–[25]. Linear functions have first been used as building block of the temporal basis functions [10], followed by the introduction of temporal basis functions with quadratic Lagrange polynomials [11]. The associated family of *shifted Lagrange basis functions* is still one of the most popular choices of temporal basis function.

The choice of temporal basis function has influence on the accuracy, efficiency, and stability of the TDIE method [6], [16]. This makes a proper design of temporal basis functions of paramount importance for the performance of MOT schemes. Temporal basis functions are constructed according to user defined design criteria. Important are efficiency, bandlimitedness, smoothness, and accuracy, which may conflict with each other. To the best of the authors' knowledge, no comprehensive analysis of the accuracy in time for MOT schemes has been given in literature.

The purpose of this paper is to define a framework for the design of temporal basis functions for use in TDIE methods, with the focus on the influence of different formulations on the accuracy of the method.

The discretization procedure in time that has been used in the MOT scheme will be interpreted as a finite element method. Intrinsic to the finite element method is the projection of the solution on a function space of finite dimension. This interpolation procedure introduces truncation errors that can be analyzed with the aid of Taylor series, resulting in clear accuracy conditions for polynomial basis functions. In this way a framework will be derived that can be used to design temporal basis functions with predefined interpolation accuracy. The well-known shifted Lagrange basis functions naturally fit in this framework, thus motivating its widespread use.

The presented framework can also be used to design novel temporal basis functions. It will be shown that smoothness

Manuscript received March 07, 2012; revised August 03, 2012; accepted August 20, 2012. Date of publication September 21, 2012; date of current version December 28, 2012.

E. van 't Wout and H. van der Ven are with the National Aerospace Laboratory NLR, Amsterdam, Netherlands (e-mail: Elwin.van.t.Wout@nlr.nl).

D. R. van der Heul and C. Vuik are with the Delft Institute of Applied Mathematics, Delft University of Technology, Delft, Netherlands.

Color versions of one or more of the figures in this paper are available online at http://ieeexplore.ieee.org.

Digital Object Identifier 10.1109/TAP.2012.2220318

can be obtained without impinging on interpolation accuracy. For instance, the cubic spline basis functions are two times continuously differentiable whereas the interpolation accuracy is the same as for cubic Lagrange basis functions. Numerical results will confirm that smoothness reduces the errors from the quadrature procedure. Surprisingly, the experimentally computed global accuracy in time for the MOT scheme using spline basis functions is orders better than for the shifted Lagrange basis functions.

The main contribution of this paper is the presentation of a careful analysis of the accuracy in time for TDIE methods. With the resulting framework, temporal basis functions can be designed with predefined accuracy and smoothness characteristics, including novel spline basis functions.

This paper will proceed as follows: Section II summarizes the model equations and its discretization, in particular the design of temporal basis functions. In Section III the interpolation error of the temporal basis functions will be analyzed. The analysis will then be used to acquire a framework for the design of temporal basis functions with specific accuracy and smoothness characteristics. The numerical results in Section IV illustrate the consequences of the various temporal basis functions on the accuracy and efficiency of the MOT scheme. Conclusions will be presented in Section V.

II. Formulation

The first part of this section summarizes the governing equations and the discretization method. Several important design criteria for temporal basis functions will be explained in the second part.

A. Time Domain Integral Equation Method

Consider a perfect electric conductor (PEC) surrounded by free space. With the Stratton-Chu formulation, backscattered fields from the object can be expressed in terms of the electric current distribution on the scattering surface. Substitution of the formulation of the scattered fields into the interface conditions results in the electric field integral equation (EFIE) and magnetic field integral equation (MFIE). The differentiated versions [1], that have no integral in time, will be used, i.e.,

$$-\mathbf{n}\times\mathbf{n}\times\int\!\!\int_\Gamma\left(\mu\frac{\ddot{\mathbf{J}}(\mathbf{r}',\tau)}{4\pi R}-\frac{1}{\epsilon}\nabla\frac{\nabla'\cdot\mathbf{J}(\mathbf{r}',\tau)}{4\pi R}\right)d\mathbf{r}' = -\mathbf{n}\times\mathbf{n}\times\dot{\mathbf{E}}^i(\mathbf{r},t) \tag{1}$$

$$\mathbf{n}\times\mathbf{n}\times\int\!\!\int_\Gamma\left(\frac{\dot{\mathbf{J}}(\mathbf{r}',\tau)}{4\pi R}+\frac{\ddot{\mathbf{J}}(\mathbf{r}',\tau)}{4\pi c}\right)\times\frac{\mathbf{R}}{R^2}\,d\mathbf{r}' - \mathbf{n}\times\frac{1}{2}\dot{\mathbf{J}}(\mathbf{r},t) = -\mathbf{n}\times\mathbf{n}\times\dot{\mathbf{H}}^i(\mathbf{r},t) \tag{2}$$

the EFIE and MFIE, respectively, which are solved for the electric surface current density $\mathbf{J}(\mathbf{r},t)$ on location $\mathbf{r}$ and time t. The dot notation $\dot{\mathbf{J}}=(\partial)/(\partial t)\mathbf{J}$ has been used for differentiation in time. The other variables are denoted as: $\mathbf{E}^i$ and $\mathbf{H}^i$ the incident electric and magnetic field, respectively, which are zero for $t<0$; $\mathbf{E}^s$ and $\mathbf{H}^s$ the scattered electric and magnetic field, respectively; Γ the scattering surface with outward pointing unit normal $\mathbf{n}$; $R=|\mathbf{R}|=|\mathbf{r}-\mathbf{r}'|$; $\tau=t-(R)/(c)$ the retarded time; and ∇ and ∇' the nabla operator with respect to $\mathbf{r}$ and $\mathbf{r}'$, respectively. The speed of light is given by $c=(\epsilon\mu)^{-(1)/(2)}$ with ϵ and μ the permittivity and permeability of free space, respectively.

The combined field integral equation (CFIE) is given by a linear combination of the EFIE (1) and MFIE (2), i.e.,

$$\mathrm{CFIE}=\frac{\kappa}{\eta}\,\mathrm{EFIE}+(1-\kappa)\,\mathrm{MFIE} \tag{3}$$

for $0\le\kappa\le 1$ and $\eta=\sqrt{\mu/\epsilon}$ the impedance [26].

Numerical discretization uses a triangular mesh on the surface Γ and a uniform partitioning in time with levels $t_k=k\Delta t$ for $k=0,1,2,\ldots,N_t$. The solution is expanded in terms of N_s spatial and N_t temporal basis functions as

$$\mathbf{J}(\mathbf{r},t)=\sum_{n=1}^{N_s}\sum_{j=0}^{N_t}J_{n,j}\mathbf{f}_n(\mathbf{r})T_j(t). \tag{4}$$

The Rao-Wilton-Glisson (RWG) functions are used for test and basis functions in space [27]. In time, collocation is performed, that is, the CFIE is point matched in subsequent time levels t_k. Temporal basis functions

$$T_j(t)=T(t-j\Delta t) \tag{5}$$

are used to interpolate the solution from discrete time levels in retarded time levels. For efficiency, causal basis functions with small support will be considered, that is, $T(t')=0$ for all $t'\le-\Delta t$ and $t'>d\Delta t$ with d a small positive integer.

The discrete CFIE can be written as a marching procedure

$$Z_0\mathbf{I}_k=\mathbf{V}_k-\sum_{j=1}^{k}Z_j\mathbf{I}_{k-j} \tag{6}$$

where $\mathbf{I}_k$ denotes the discrete surface current density at time t_k, $\mathbf{V}_k$ the incident field at time t_k, and Z_j discrete interaction matrices [6]. At every time level k the discrete surface current density can be calculated from known solutions only, resulting in the Marching-on-in-Time scheme.

B. Temporal Basis Functions

The choice of the temporal basis function (5) is the topic of this paper. The present analysis will only make use of temporal basis functions that result in efficient MOT schemes and which can be designed with conditions on accuracy and smoothness.

Efficiency of a numerical scheme is given by the trade-off between the amount of work and accuracy. Generally speaking, a temporal basis function with small support results in an inexpensive TDIE method whereas a large support results in an accurate method [28], [29]. In order to obtain the fast MOT algorithm (6), causal basis functions with small support will be used. These compact temporal basis function are not bandlimited [6].

Accuracy and smoothness will be the main guidelines in the present design of temporal basis functions. Accuracy of the MOT scheme depends on various errors, including spatial discretization error, temporal discretization error, and quadrature error. The different errors are coupled due to the presence of retarded time levels in the CFIE. A higher order of accuracy may be advantageous because less stringent requirements have to be imposed on the mesh size for the same truncation error.

The temporal discretization error will be isolated in this paper to enable concise derivations of the design criteria. The present analysis considers the interpolation error of temporal basis function as a measure of temporal discretization error. This results in expressions of the order of interpolation accuracy with respect to the size of support of the temporal basis functions.

The quadrature error originates from the numerical integration in space of surface currents in retarded time levels. Smoothness of temporal basis functions is likely to improve the quadrature accuracy. Piecewise polynomial temporal basis functions will be considered because analytical expressions of the spatial integrals are available [5], [30]. These quasi-exact methods improve the integration accuracy considerably but are nontrivial to implement and preclude extension to spatial curvilinear elements.

For these reasons, the present analysis restricts to temporal basis functions (5) that are defined by piecewise polynomials which have a small support and are causal. They can conveniently be written as

$$T(t) = \begin{cases} F_0(t), & -1 < \tilde{t} \leq 0 \\ F_1(t), & 0 < \tilde{t} \leq 1 \\ \vdots & \vdots \\ F_d(t), & d-1 < \tilde{t} \leq d \\ 0, & \text{else} \end{cases} \tag{7}$$

with $F_0, F_1, \ldots, F_d$ polynomials of degree d, and $\tilde{t} = (t)/(\Delta t)$ the scaled time.

III. Accuracy Design of Temporal Basis Functions

The CFIE (3) has been discretized with the MOT scheme. To isolate the properties of the time components, the spatially discretized CFIE will be considered. This is a delay differential equation in time that uses both the first and second derivative. Its solution is a time-dependent vector that corresponds to the electric surface current density on the spatial mesh.

The discretization procedure in time of the MOT scheme will be analyzed with the theory of finite element methods [31]. An analysis of the interpolation procedure results in a framework for the design of temporal basis functions with a predefined order of interpolation accuracy. Additional requirements on the smoothness yield various temporal basis functions, including shifted Lagrange and spline basis functions.

Evidently, the accuracy of interpolation has influence on the global accuracy of the MOT scheme. However, it is not necessary that the orders of interpolation and global accuracy are exactly the same. In Section IV the global accuracy will be analyzed experimentally for a number of different temporal basis functions that can be defined within the current framework.

A. Interpolation

In finite element methods the solution of a differential equation is approximated in a finite dimensional subspace. The map of the solution onto the finite element space is called *interpolation* and is one of the sources of discretization errors. Temporal basis functions determine the finite element space and the accuracy of interpolation. A thorough analysis of the interpolation procedure will result in clear conditions on temporal basis functions for small interpolation errors.

For an arbitrary function $u(t)$ the interpolator $\mathcal{I}$ defines the interpolant $\hat{u}(t)$ by

$$\hat{u} = \mathcal{I}(u) = \sum_{j=1}^{N} \tilde{u}_j T_j \tag{8}$$

for coefficients $\tilde{u}_j$ which will be defined later and $T_j(t)$ temporal basis functions (5). The interpolation error is given by $\|u - \mathcal{I}u\|$ where the type of norm will be specified later. Recall that for the CFIE the first and second time derivative have to be evaluated in the retarded time as well. Therefore, the interpolation errors $\|u' - \mathcal{I}u'\|$ and $\|u'' - \mathcal{I}u''\|$ are also of interest. The derivative of a function is interpolated with the derivative of the same basis functions, i.e.,

$$\mathcal{I}u' = \sum_{j=1}^{N} \tilde{u}_j T_j' \tag{9}$$

$$\mathcal{I}u'' = \sum_{j=1}^{N} \tilde{u}_j T_j''. \tag{10}$$

For a correct interpolation procedure, two choices have to be made, namely the definition of the finite element space and the map onto this space. Since basis functions in the form of (7) are used, the finite element space is defined by the space of piecewise polynomials of degree d. The map onto the finite element space is based on the definition of the coefficients $\tilde{u}_j$ that depend on u, i.e.,

$$\tilde{u}_j = \mathcal{N}_j(u) \tag{11}$$

for a functional $\mathcal{N}_j$, called a *nodal variable* [31]. This nodal variable should be chosen such that the interpolation can be analyzed easily. Additionally, a natural requirement is that the well-known shifted Lagrange basis functions should fit within this choice for the nodal variables.

It is common practice to use an interpolation that is a projection. A sufficient condition is $\mathcal{N}_i(T_j) = \delta_{ij}$ for $i, j = 1, 2, \ldots, N$ with δ_{ij} denoting the Kronecker delta. For the nodal variables and temporal basis functions that will be used in this paper, this condition is satisfied a posteriori.

B. Quadratic Basis Functions

Consider temporal basis functions based on quadratic polynomials. For an arbitrary time point τ, satisfying $t_{\ell-1} < \tau \leq t_\ell$, the interpolant (8) reads

$$\mathcal{I}u(\tau) = \sum_{j=1}^{N} \tilde{u}_j T_j(\tau) = \sum_{k=0}^{2} \tilde{u}_{\ell-k} F_k(k\Delta t - \sigma) \tag{12}$$

with F_k as defined in (7). The pointwise interpolation error

$$\|u - \mathcal{I}u\| = |u(\tau) - \mathcal{I}u(\tau)| \tag{13}$$

will be used to analyze the accuracy of the interpolation. The coefficients $\tilde{u}_{\ell-k}$ that determine the interpolation are defined by (11). As nodal variable, use

$$\mathcal{N}_j(u) = u(t_j) + \alpha \Delta t u'(t_j) \tag{14}$$

for a constant α. This choice allows a straightforward analysis of the interpolation accuracy by using Taylor series. The inter-

polant can then be written in terms of the unknown solution in the arbitrary time point τ.

Quadratic polynomials may lead to an interpolation that is third order accurate [31], to be precise,

$$|u(\tau) - \hat{u}(\tau)| = \mathcal{O}(\Delta t^3). \tag{15}$$

To obtain this accuracy temporal basis functions have to satisfy

$$F_{0,\sigma} + F_{1,\sigma} + F_{2,\sigma} = 1 \tag{16}$$

$$F_{1,\sigma} + 2F_{2,\sigma} = \frac{\sigma}{\Delta t} + \alpha \tag{17}$$

$$F_{1,\sigma} + 4F_{2,\sigma} = \frac{\sigma^2}{\Delta t^2} + 2\alpha\frac{\sigma}{\Delta}t + 2\alpha^2 \tag{18}$$

for $F_{0,\sigma} = F_0(-\sigma)$, $F_{1,\sigma} = F_1(\Delta t - \sigma)$, and $F_{2,\sigma} = F_2(2\Delta t - \sigma)$, as derived in the Appendix. The first equation is the well-known unit sum condition for interpolants. Recall that the first and second derivative have to be interpolated as well. Since the derivatives of the same basis function are used, the interpolation of the derivatives are based on polynomials of a lower degree. This reduces the accuracy of interpolation for the derivatives, to be precise,

$$|u'(\tau) - \hat{u}'(\tau)| = \mathcal{O}(\Delta t^2) \tag{19}$$

$$|u''(\tau) - \hat{u}''(\tau)| = \mathcal{O}(\Delta t). \tag{20}$$

The interpolation for the CFIE is thus first order accurate.

To obtain the claimed orders of interpolation accuracy, the temporal basis function has to satisfy conditions (16)–(18). This system of three equations can be solved uniquely as

$$T(t) = \begin{cases} \frac{1}{2}\tilde{t}^2 + \left(\frac{3}{2} - \alpha\right)\tilde{t} + \alpha^2 - \frac{3}{2}\alpha + 1, & -1 < \tilde{t} \leq 0 \\ -\tilde{t}^2 + 2\alpha\tilde{t} - 2\alpha^2 + 1, & 0 < \tilde{t} \leq 1 \\ \frac{1}{2}\tilde{t}^2 - \left(\frac{3}{2} + \alpha\right)\tilde{t} + \alpha^2 + \frac{3}{2}\alpha + 1, & 1 < \tilde{t} \leq 2 \\ 0, & \text{else.} \end{cases} \tag{21}$$

For any constant α this temporal basis function results in a first order accurate interpolation of the CFIE. A sophisticated choice of α can be made by requiring a continuous basis function. When α satisfies

$$\alpha\left(\alpha - \frac{1}{2}\right) = 0 \tag{22}$$

the temporal basis function will be continuous. The two solutions $\alpha = 0$ and $\alpha = (1)/(2)$ can be substituted into the general representation (21) of the temporal basis function. The choice of $\alpha = 0$ results in

$$T(t) = \begin{cases} \frac{1}{2}\tilde{t}^2 + \frac{3}{2}\tilde{t} + 1, & -1 < \tilde{t} \leq 0 \\ -\tilde{t}^2 + 1, & 0 < \tilde{t} \leq 1 \\ \frac{1}{2}\tilde{t}^2 - \frac{3}{2}\tilde{t} + 1, & 1 < \tilde{t} \leq 2 \\ 0, & \text{else} \end{cases} \tag{23}$$

which can be recognized as the quadratic Lagrange basis function [11]. The choice of $\alpha = (1)/(2)$ results in

$$T(t) = \begin{cases} \frac{1}{2}\tilde{t}^2 + \tilde{t} + \frac{1}{2} & -1 < \tilde{t} \leq 0 \\ -\tilde{t}^2 + \tilde{t} + \frac{1}{2} & 0 < \tilde{t} \leq 1 \\ \frac{1}{2}\tilde{t}^2 - 2\tilde{t} + 2 & 1 < \tilde{t} \leq 2 \\ 0 & \text{else.} \end{cases} \tag{24}$$

This is the temporal basis function based on quadratic B-splines [20], [21]. Although only continuity has been required, the spline basis function has a continuous derivative as well.

C. Cubic Basis Functions

To increase the interpolation accuracy of the MOT scheme cubic basis functions can be used, since cubic polynomials may result in fourth order accurate interpolation [31]. The derivation of temporal basis functions that satisfy this accuracy will be analogous to the derivation for quadratic basis functions.

The nodal variable that will characterize the basis functions is chosen to be

$$\mathcal{N}_j(u) = u(t_j) + \alpha\Delta t u'(t_j) + \beta\Delta t^2 u''(t_j) \tag{25}$$

for constants α and β. For cubic polynomials one can obtain fourth order accurate interpolation. The differentiated functions in the CFIE are interpolated with lower order polynomials and therefore a lower order of accuracy can be obtained. So, an interpolation procedure is searched for that satisfies

$$|u(\tau) - \hat{u}(\tau)| = \mathcal{O}(\Delta t^4) \tag{26}$$

$$|u'(\tau) - \hat{u}'(\tau)| = \mathcal{O}(\Delta t^3) \tag{27}$$

$$|u''(\tau) - \hat{u}''(\tau)| = \mathcal{O}(\Delta t^2). \tag{28}$$

With a straightforward extension of the derivation in the Appendix, it can be shown that cubic polynomial basis functions have to satisfy

$$F_{0,\sigma} + F_{1,\sigma} + F_{2,\sigma} + F_{3,\sigma} = 1 \tag{29}$$

$$F_{1,\sigma} + 2F_{2,\sigma} + 3F_{3,\sigma} = \frac{\sigma}{\Delta t} + \alpha \tag{30}$$

$$F_{1,\sigma} + 4F_{2,\sigma} + 9F_{3,\sigma} = \frac{\sigma^2}{\Delta t^2} + 2\alpha\frac{\sigma}{\Delta t} + 2(\alpha^2 - \beta) \tag{31}$$

$$F_{1,\sigma} + 8F_{2,\sigma} + 27F_{3,\sigma} = \frac{\sigma^3}{\Delta t^3} + \frac{\alpha}{2}\frac{\sigma^2}{\Delta t^2} + (\alpha^2 - \beta)\frac{\sigma}{\Delta t} + \alpha^3 - 2\alpha\beta. \tag{32}$$

This system of equations can be solved uniquely as

$$F_0(t) = \frac{1}{6}\tilde{t}^3 + \left(1 - \frac{1}{2}\alpha\right)\tilde{t}^2 + \left(\frac{11}{6} + \alpha^2 - 2\alpha - \beta\right)\tilde{t} + 1 - \alpha^3 + 2\alpha^2 - \frac{11}{6}\alpha + 2\alpha\beta - 2\beta \tag{33}$$

$$F_1(t) = -\frac{1}{2}\tilde{t}^3 - \left(1 - \frac{3}{2}\alpha\right)\tilde{t}^2 + \left(\frac{1}{2} - 3\alpha^2 + 2\alpha + 3\beta\right)\tilde{t} + 1 + 3\alpha^3 - 2\alpha^2 - \frac{1}{2}\alpha - 6\alpha\beta + 2\beta \tag{34}$$

$$F_2(t) = \frac{1}{2}\tilde{t}^3 - \left(1 + \frac{3}{2}\alpha\right)\tilde{t}^2 - \left(\frac{1}{2} - 3\alpha^2 - 2\alpha + 3\beta\right)\tilde{t} + 1 - 3\alpha^3 - 2\alpha^2 + \frac{1}{2}\alpha + 6\alpha\beta + 2\beta \tag{35}$$

$$F_3(t) = -\frac{1}{6}\tilde{t}^3 + \left(1+\frac{1}{2}\alpha\right)\tilde{t}^2 - \left(\frac{11}{6}+\alpha^2+2\alpha-\beta\right)\tilde{t} + 1+\alpha^3+2\alpha^2+\frac{11}{6}\alpha-2\alpha\beta-2\beta. \quad (36)$$

This general representation of temporal basis functions still has the freedom to choose the parameters α and β. Some choices of the parameters result in temporal basis functions that can be found in literature [21]. However, to the best of the authors' knowledge, this family of temporal basis function has not been given in literature and therefore novel temporal basis functions can be designed readily. The specific choices made in this paper will be based on requirements on smoothness.

Requiring a continuous temporal basis function results in the condition

$$\alpha^3 - \alpha^2 + \frac{1}{3}\alpha - 2\alpha\beta + \beta = 0. \quad (37)$$

When one requires a continuous derivative, the condition

$$\frac{1}{3} + \alpha^2 - \alpha - \beta = 0 \quad (38)$$

has to be satisfied. Temporal basis functions that are $\mathcal{C}^1(\mathbb{R})$ continuous have to satisfy both conditions (37) and (38). Its unique real-valued solution is $(\alpha,\beta) = (1,(1/3))$. For this choice of parameters, the temporal basis function reads

$$T(t) = \begin{cases} \frac{1}{6}\tilde{t}^3 + \frac{1}{2}\tilde{t}^2 + \frac{1}{2}\tilde{t} + \frac{1}{6}, & -1 < \tilde{t} \le 0 \\ -\frac{1}{2}\tilde{t}^3 + \frac{1}{2}\tilde{t}^2 + \frac{1}{2}\tilde{t} + \frac{1}{6}, & 0 < \tilde{t} \le 1 \\ \frac{1}{2}\tilde{t}^3 - \frac{5}{2}\tilde{t}^2 + \frac{7}{2}\tilde{t} - \frac{5}{6}, & 1 < \tilde{t} \le 2 \\ -\frac{1}{6}\tilde{t}^3 + \frac{3}{2}\tilde{t}^2 - \frac{9}{2}\tilde{t} + \frac{9}{2}, & 2 < \tilde{t} \le 3 \\ 0, & \text{else.} \end{cases} \quad (39)$$

Although only $\mathcal{C}^1(\mathbb{R})$ continuity has been required, it is in fact $\mathcal{C}^2(\mathbb{R})$ continuous. Therefore, it is called the *cubic spline basis function*. This temporal basis function results in a second order accurate interpolation procedure for the CFIE and has the striking feature of being $\mathcal{C}^2$ continuous.

Alleviating the smoothness requirement makes it possible to design different basis functions. For continuity, condition (37) on α and β is the only one and has infinitely many solutions. Recall that the nodal variable (25) has been chosen such that well-known basis functions can be obtained. To show this capability of the framework, consider the solution $(\alpha,\beta) = (0,0)$. This choice results in

$$T(t) = \begin{cases} \frac{1}{6}\tilde{t}^3 + \tilde{t}^2 + \frac{11}{6}\tilde{t} + 1, & -1 < \tilde{t} \le 0 \\ -\frac{1}{2}\tilde{t}^3 - \tilde{t}^2 + \frac{1}{2}\tilde{t} + 1, & 0 < \tilde{t} \le 1 \\ \frac{1}{2}\tilde{t}^3 - \tilde{t}^2 - \frac{1}{2}\tilde{t} + 1, & 1 < \tilde{t} \le 2 \\ -\frac{1}{6}\tilde{t}^3 + \tilde{t}^2 - \frac{11}{6}\tilde{t} + 1, & 2 < \tilde{t} \le 3 \\ 0, & \text{else} \end{cases} \quad (40)$$

which is the cubic Lagrange basis function [15].

The various temporal basis functions introduced in this section are depicted in Fig. 1 and their properties are summarized in Table I.

In this section, quadratic and cubic temporal basis functions have been designed that result in an interpolation procedure for the CFIE with first and second order accuracy, respectively. The current framework can readily be extended to higher order polynomials with larger support. The natural extension of the nodal variable is to include higher order derivatives. These extensions introduce more degrees of freedom for the design of temporal basis functions. As is derived in this paper, higher orders of interpolation accuracy or better smoothness characteristics can be obtained. However, the degrees of freedom can also be used to fulfill other types of design criteria. For instance, the choice of temporal basis function has an effect on the efficiency of the linear solver. In every iteration of the MOT scheme (6) a system of linear equations has to be solved, which is computationally expensive for large condition numbers. The shape of the temporal basis function has influence on the condition number of discretization matrices. Further research is required to derive concise conditions on these degrees of freedom.

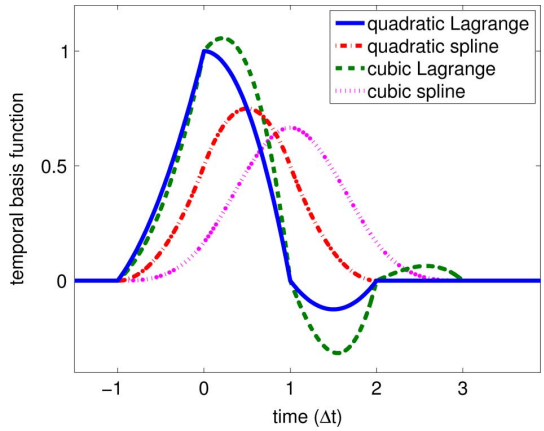

Fig. 1. The shape of the temporal basis functions.

TABLE I
INTERPOLATION ACCURACY FOR THE THREE TEMPORAL TERMS, THE TOTAL INTERPOLATION ACCURACY OF THE CFIE AND THE SMOOTHNESS OF THE VARIOUS TEMPORAL BASIS FUNCTIONS

tbf	acc. T	acc. T'	acc. T''	total acc.	smoothness
qL	$\mathcal{O}(\Delta t^3)$	$\mathcal{O}(\Delta t^2)$	$\mathcal{O}(\Delta t)$	$\mathcal{O}(\Delta t)$	$\mathcal{C}^0(\mathbb{R})$
qs	$\mathcal{O}(\Delta t^3)$	$\mathcal{O}(\Delta t^2)$	$\mathcal{O}(\Delta t)$	$\mathcal{O}(\Delta t)$	$\mathcal{C}^1(\mathbb{R})$
cL	$\mathcal{O}(\Delta t^4)$	$\mathcal{O}(\Delta t^3)$	$\mathcal{O}(\Delta t^2)$	$\mathcal{O}(\Delta t^2)$	$\mathcal{C}^0(\mathbb{R})$
cs	$\mathcal{O}(\Delta t^4)$	$\mathcal{O}(\Delta t^3)$	$\mathcal{O}(\Delta t^2)$	$\mathcal{O}(\Delta t^2)$	$\mathcal{C}^2(\mathbb{R})$

IV. EXPERIMENTAL VERIFICATION

Four temporal basis functions have been designed with the presented framework. In this section, the implications of the different smoothness and accuracy characteristics on the performance of the MOT scheme will be verified experimentally. Particularly, the effect of smoothness on the quadrature accuracy and the effect of interpolation accuracy on global accuracy in time will be analyzed.

Two test cases will be considered, namely a cube with edges of 1 m and a sphere with a diameter of 1 m. As depicted in Fig. 2, the cube and sphere are partitioned into 480 and 238 triangular patches, respectively. A Gaussian plane wave

$$\mathbf{E}^i(\mathbf{r},t) = 120\pi\mathbf{p}\frac{4}{\sqrt{\pi}T}e^{-(4(c(t-t_0)-\mathbf{r}\cdot\mathbf{k})/T)^2} \quad (41)$$

will be used as incident field, with the parameters given by: polarization $\mathbf{p} = \tilde{\mathbf{x}}$, propagation $\mathbf{k} = -\tilde{\mathbf{z}}$, pulse width $T = 6$ lm, and pulse delay $t_0 = 4$ lm. To get an equal contribution from the EFIE and MFIE, the CFIE-0.5 will be used, i.e., $\kappa = 0.5$ in

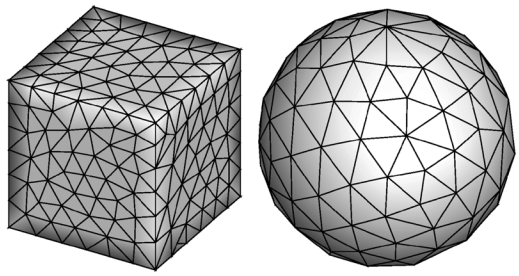

Fig. 2. The mesh of the cube and sphere used as test problem.

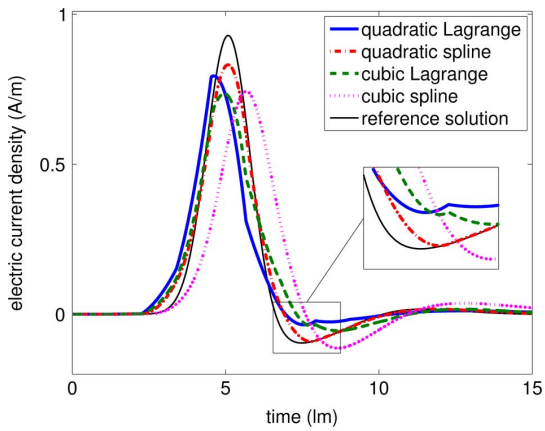

Fig. 3. Electric surface current density at the top face of the sphere.

(3). If not specified, the outer spatial integral has been calculated with Gaussian quadrature with 7 points on each triangle patch and the inner integral calculated analytically [30].

A. Smoothness

An important feature of the spline basis functions (24) and (39) is the continuous derivative on the whole time axis whereas shifted Lagrange basis functions (23) and (40) are only continuous. The discrete surface current density calculated with the spline basis functions is therefore expected to be smooth. To verify this implication, the TDIE method will be used with a large time step size, for which the effect of smooth basis functions on the solution will appear. For the sphere and cube a time step size of 1.13 lm and 0.71 lm has been used. As a reference solution, the MOT scheme has been applied with a small time step size of 0.014 lm and 0.029 lm for the sphere and cube, respectively. The results depicted in Figs. 3 and 4 clearly show that the smoothness properties of the temporal basis functions lead to similar smoothness properties of the discrete electric surface current density.

B. Accuracy

The global accuracy of TDIE methods depends on different kinds of numerical errors. Important sources of errors are

- spatial discretization,
- temporal discretization,
- quadrature integration, and
- solution of the system of discretized equations.

Spatial discretization errors originate from the representation of electric surface currents on an object by RWG functions on a

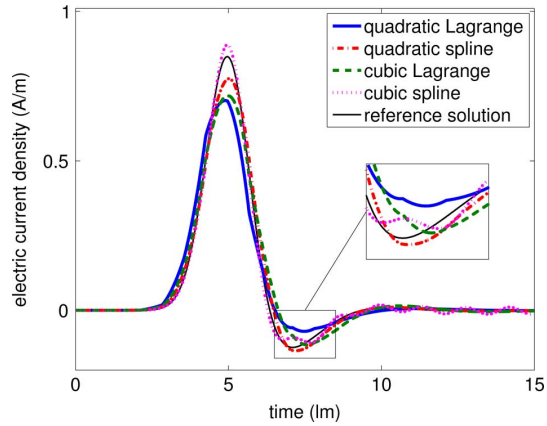

Fig. 4. Electric surface current density at the top face of the cube.

surface mesh. The analysis of these errors is outside the scope of this paper. The temporal discretization error has been analyzed in Section III by deriving error bounds on the interpolation error of temporal basis functions. Quadrature errors are present since the spatial integrals are computed with a quadrature procedure on the triangular elements. The errors from solving the discrete system can be neglected because an LU decomposition has been used as linear solver.

Below, the quadrature and interpolation accuracy will be considered in more detail.

1) Quadrature Accuracy: The CFIE (3) is given by spatial integrals over the triangular surface mesh. Gaussian quadrature has been used to evaluate the integrals, which is effective for smooth integrands. The integrands in the CFIE depend on the temporal basis functions evaluated in retarded time levels. Smooth temporal basis functions therefore yield integrands that are smooth in space and the quadrature accuracy is expected to improve.

Recall that the quadrature procedure is applied to the outer integral only because the inner integral has been calculated with analytic expressions [30]. As test problem the sphere has been used with a time step size of 0.14 lm.

The discretized EFIE (1) consists of the terms

$$V^q_{mn,j} = \int\!\!\int_{\Gamma_q} \mathbf{f}_m(\mathbf{r}) \cdot \int\!\!\int_{\Gamma} \frac{\mathbf{f}_n(\mathbf{r}')\ddot{T}_j(\tau)}{4\pi R} d\mathbf{r}' d\mathbf{r} \tag{42}$$

$$S^q_{mn,j} = \int\!\!\int_{\Gamma_q} \nabla \cdot \mathbf{f}_m(\mathbf{r}) \int\!\!\int_{\Gamma} \frac{\nabla' \cdot \mathbf{f}_n(\mathbf{r}')T_j(\tau)}{4\pi R} d\mathbf{r}' d\mathbf{r} \tag{43}$$

that can be related with the magnetic vector and scalar potential, respectively [10]. Γ_q denotes the surface mesh with q quadrature points on each triangular patch. Notice that the value j determines the matrix Z_j in the MOT scheme (6) of which the discrete terms are an element. For each temporal basis function, both terms will be computed with different numbers of quadrature points. The convergence towards the reference experiment with 73 quadrature points will be considered. The relative error is therefore defined as

$$\frac{\|V^q_{mn,j} - V^{73}_{mn,j}\|}{\|V^{73}_{mn,j}\|}.$$

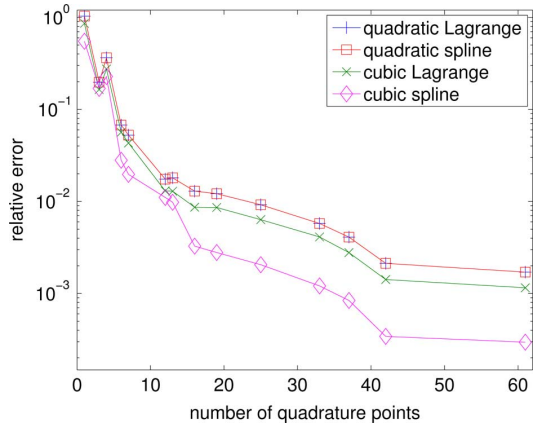

Fig. 5. Relative error for the vector potential term on a sphere.

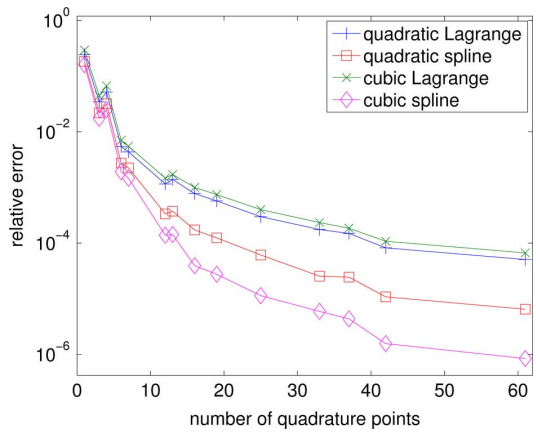

Fig. 6. Relative error for the scalar potential term on a sphere.

For a given j, the ℓ^2 norm

$$\|V_{mn,j}\|^2 = \sum_{m=1}^{N_s}\sum_{n=1}^{N_s}|V_{mn,j}|^2$$

over all edge pairs has been used. The convergence results for the vector potential term (42) is depicted in Fig. 5 with $j = 3$ and for the scalar potential term (43) in Fig. 6 with $j = 6$.

For the cubic basis functions, the smoothness of the spline basis function indeed improves the convergence as depicted in Fig. 5. For the quadratic basis functions, however, exactly the same convergence is observed. This is expected because the vector potential term (42) contains $\ddot{T}$ only, which is the same for both quadratic Lagrange and spline basis function.

Because the scalar potential term does not have a time derivative, the smoothness properties of the temporal basis functions are all different. Fig. 6 clearly shows that smoothness of the temporal basis function improves the convergence with respect to the number of quadrature points.

The positive influence of smooth basis functions on the quadrature accuracy of the discrete terms has been verified experimentally. But a faster convergence for the elements of the interaction matrices does not necessarily imply more accurate solutions of the MoT scheme. It is therefore not evident that smoothness of temporal basis functions will also have a positive influence on the discrete surface current density of the TDIE method.

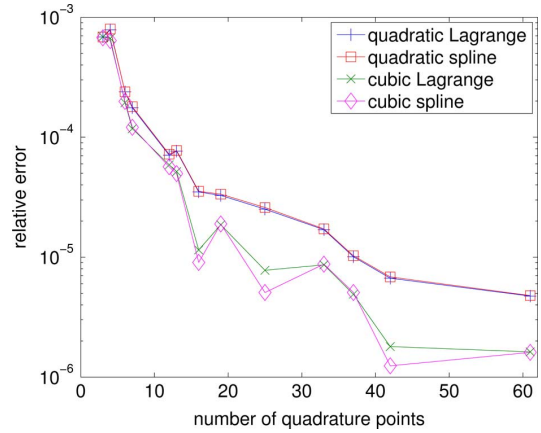

Fig. 7. Relative error for the electric surface current density on a sphere.

TABLE II
EXPERIMENTAL ORDER OF INTERPOLATION ACCURACY

temporal basis function	u	u'	u''
quadratic Lagrange	3.000	1.994	0.995
quadratic spline	3.000	2.005	1.000
cubic Lagrange	3.999	2.990	1.992
cubic spline	3.999	3.085	2.001

The solution of the EFIE has been computed with the MOT scheme for different numbers of quadrature points. The convergence towards the reference solution for 73 quadrature points will be considered. The relative error is given by

$$\frac{\|J^q_{n,j} - J^{73}_{n,j}\|}{\|J^{73}_{n,j}\|}$$

where $J^q_{n,j}$ denotes the coefficients in (4) computed with q quadrature points. The norm is defined in both discrete space and time as

$$\|J_{n,j}\|^2 = \sum_{n=1}^{N_s}\sum_{j=1}^{100}|J_{n,j}|^2.$$

The convergence results depicted in Fig. 7 show a faster convergence for spline basis functions compared to shifted Lagrange basis functions of equal support. For this specific test case, the increase in convergence rate for the surface current density is not as prominent as for the matrix elements.

2) Interpolation Accuracy: In this paper, the accuracy in time of the MOT scheme has been analyzed by deriving bounds on the interpolation error, as summarized in Table I. To validate the analysis, a given function will be interpolated, for instance a Gaussian curve $u(t) = e^{-(12t-6)^2}$ for $0 \le t \le 1$. The interpolant (8) calculated with a time step size $\Delta t = 1/800$ is denoted by $\hat{u}_1$ and with $\Delta t = 1/400$ by $\hat{u}_2$. Then the order of interpolation accuracy can be computed as $\log_2((\|\hat{u}_2 - u\|)/(\|\hat{u}_1 - u\|))$ and similar for the derivatives. Results with the L^2 norm are given in Table II. The experimental accuracy perfectly matches the expected accuracy.

TABLE III
EXPERIMENTAL ORDER OF ACCURACY ON A SPHERE, WITH THE SMALLEST TIME STEP SIZE LISTED

temporal basis function	0.014 lm	0.028 lm	0.043 lm	0.057 lm
quadratic Lagrange	1.039	1.085	1.129	1.166
quadratic spline	1.982	2.017	2.005	1.992
cubic Lagrange	2.044	2.093	2.135	2.159
cubic spline	4.079	4.229	4.028	4.016

TABLE IV
EXPERIMENTAL ORDER OF ACCURACY ON A CUBE, WITH THE SMALLEST TIME STEP SIZE LISTED

temporal basis function	0.012 lm	0.023 lm	0.035 lm	0.047 lm
quadratic Lagrange	1.004	1.014	1.018	1.030
quadratic spline	1.996	2.004	1.989	2.044
cubic Lagrange	2.011	2.027	2.035	2.038
cubic spline	4.133	3.611	4.047	4.551

3) Global Accuracy: The global accuracy in time of TDIE methods depends on the interpolation accuracy but does not necessarily have to satisfy the same orders of accuracy. With Richardson's extrapolation algorithm the global accuracy can be investigated experimentally. Consider three experiments with three different time step sizes, all on the same spatial mesh. The x-component of the discrete electric surface current density on top of the object is denoted by $J_1(t)$, $J_2(t)$, and $J_4(t)$, for time step sizes Δt, $2\Delta t$, and $4\Delta t$, respectively. The order of the global accuracy in time can be computed as $\log_2((\|J_4 - J_2\|)/(\|J_2 - J_1\|))$ where the L^2 norm has been used for $0 \leq t \leq 14$ lm. The results for the sphere and cube are listed in Tables III and IV, respectively.

For the shifted Lagrange basis functions the experimental order of accuracy converges to the expected $\mathcal{O}(\Delta t)$ and $\mathcal{O}(\Delta t^2)$ for the quadratic and cubic version, respectively. However, a global error of $\mathcal{O}(\Delta t^2)$ and $\mathcal{O}(\Delta t^4)$ is observed for the quadratic and cubic spline basis function, respectively. Apparently, the interpolation error does not restrict the global accuracy when the spline basis functions are used and higher orders of accuracy are obtained. The smoothness of the temporal basis functions probably results in the higher orders of accuracy. The actual cause of this remarkably better accuracy for the spline basis functions is a topic for future research.

The focus of this paper has been on accuracy and smoothness of MoT schemes. Numerical stability is also an important property of computational methods. Our experiments indicate that cubic spline basis functions are more prone to late-time instability than Lagrange functions. This sounds counterintuitive, since smoothness is expected to improve stability [6]. Due to the shifted weights of the cubic spline basis function, more importance is given to past influences instead of immediate interactions. The weaker diagonal dominance of the leading matrix in the marching algorithm (6) possibly leads to accumulating numerical errors. On the positive side, quadratic spline basis functions result in stable solutions. The extension to stability of this framework for the design temporal basis functions is a topic of further research.

V. CONCLUSION

In this paper a framework has been derived to design temporal basis functions with predefined interpolation accuracy. This results in spline basis functions that have the same interpolation accuracy and have better smoothness properties compared to shifted Lagrange basis functions. Numerical experiments show a higher order of global accuracy for the spline basis functions than for the shifted Lagrange basis functions with equal support.

APPENDIX
DERIVATION OF THE ACCURACY CONDITIONS

Temporal basis functions in the MOT scheme are denoted by $T_j(t)$ and formulated as $T_j(t) = T(t - j\Delta T)$. The definition of T will then give a representation of all temporal basis functions. The class of causal basis functions with a small support can be written as

$$T(t) = \begin{cases} F_0(t), & -\Delta t < t \leq 0 \\ F_1(t), & 0 < t \leq \Delta t \\ F_2(t), & \Delta t < t \leq 2\Delta t \\ 0, & \text{else} \end{cases} \tag{44}$$

for F_0, F_1, and F_2 denoting quadratic polynomials and Δt the time step size. Consider an arbitrary retarded time level τ_k, for which one can find a discrete time level $t_\ell = \ell\Delta t$ such that $t_{\ell-1} < \tau_k \leq t_\ell$. With σ defined as $\sigma = t_\ell - \tau_k$, the analysis can be restricted to an arbitrary $\sigma \in [0, \Delta t)$.

The unknown solution of the spatially discretized CFIE in the MOT scheme is denoted by $u(t)$. This solution is mapped towards a finite dimensional space that include all temporal basis functions. The solution inside this finite element space is denoted by $\hat{u}(t)$ and is defined by a series expansion in terms of temporal basis functions $T_j(t)$ as

$$\hat{u}(t) = \sum_{j=1}^{N} \tilde{u}_j T_j(t). \tag{45}$$

The coefficients $\tilde{u}_j$ are defined by a nodal variable $\mathcal{N}_j$. In this case, use

$$\tilde{u}_j = \mathcal{N}_j(u) = u(t_j) + \alpha\Delta t u'(t_j) \tag{46}$$

for a constant α. For the derivatives of the solution, the derivative of the temporal basis functions are used, i.e.,

$$\hat{u}'(t) = \sum_{j=1}^{N} \tilde{u}_j T_j'(t) \text{ and } \hat{u}''(t) = \sum_{j=1}^{N} \tilde{u}_j T_j''(t).$$

For quadratic polynomial basis functions (44) the interpolation procedure results in

$$\begin{aligned} \hat{u}(\tau_k) = {} & F_0(-\sigma)\tilde{u}_\ell + F_1(\Delta t - \sigma)\tilde{u}_{\ell-1} \\ & + F_2(2\Delta t - \sigma)\tilde{u}_{\ell-2} \end{aligned} \tag{47}$$

$$\begin{aligned} \hat{u}'(\tau_k) = {} & F_0'(-\sigma)\tilde{u}_\ell + F_1'(\Delta t - \sigma)\tilde{u}_{\ell-1} \\ & + F_2'(2\Delta t - \sigma)\tilde{u}_{\ell-2} \end{aligned} \tag{48}$$

$$\begin{aligned} \hat{u}''(\tau_k) = {} & F_0''(-\sigma)\tilde{u}_\ell + F_1''(\Delta t - \sigma)\tilde{u}_{\ell-1} \\ & + F_2''(2\Delta t - \sigma)\tilde{u}_{\ell-2}. \end{aligned} \tag{49}$$

The interpolation error of $\hat{u}$, $\hat{u}'$, and $\hat{u}''$ at an arbitrary retarded time level is given by $|\hat{u}(\tau_k)-u_\sigma|$, $|\hat{u}'(\tau_k)-u'_\sigma|$, and $|\hat{u}''(\tau_k)-u''_\sigma|$, respectively, for $u_\sigma = u(\tau_k)$, $u'_\sigma = u'(\tau_k)$, and $u''_\sigma = u''(\tau_k)$. To obtain the interpolation accuracy, the coefficients are written as a Taylor series in the unknown functions in the retarded time level. That is,

$$\tilde{u}_\ell = u_\sigma + \sigma u'_\sigma + \frac{1}{2}\sigma^2 u''_\sigma + \alpha\Delta t u'_\sigma + \alpha\Delta t\sigma u''_\sigma + \mathcal{O}(\Delta t^3) \quad (50)$$

$$\tilde{u}_{\ell-1} = u_\sigma + (\sigma-\Delta t)u'_\sigma + \frac{1}{2}(\sigma-\Delta t)^2 u''_\sigma + \alpha\Delta t u'_\sigma + \alpha\Delta t(\sigma-\Delta t)u''_\sigma + \mathcal{O}(\Delta t^3) \quad (51)$$

$$\tilde{u}_{\ell-1} = u_\sigma + (\sigma-2\Delta t)u'_\sigma + \frac{1}{2}(\sigma-2\Delta t)^2 u''_\sigma + \alpha\Delta t u'_\sigma + \alpha\Delta t(\sigma-2\Delta t)u''_\sigma + \mathcal{O}(\Delta t^3) \quad (52)$$

since $\mathcal{O}(\sigma) = \mathcal{O}(\Delta t)$. Substitution of the Taylor series (50)–(52) into the interpolants (47)–(49) results in

$$\hat{u}(\tau_k) = \mathcal{A}_{11}u_\sigma + \mathcal{A}_{12}u'_\sigma + \mathcal{A}_{13}u''_\sigma + \mathcal{O}(\Delta t^3) \quad (53)$$

$$\hat{u}'(\tau_k) = \mathcal{A}_{21}u_\sigma + \mathcal{A}_{22}u'_\sigma + \mathcal{A}_{23}u''_\sigma + \mathcal{O}(\Delta t^2) \quad (54)$$

$$\hat{u}''(\tau_k) = \mathcal{A}_{31}u_\sigma + \mathcal{A}_{32}u'_\sigma + \mathcal{A}_{33}u''_\sigma + \mathcal{O}(\Delta t) \quad (55)$$

with $\mathcal{A}_{ij}$ given by

$$\mathcal{A}_{11} = F_{0,\sigma} + F_{1,\sigma} + F_{2,\sigma} \quad (56)$$

$$\mathcal{A}_{12} = (\sigma+\alpha\Delta t)F_{0,\sigma} + (\sigma+(\alpha-1)\Delta t)F_{1,\sigma} + (\sigma+(\alpha-2)\Delta t)F_{2,\sigma} \quad (57)$$

$$\mathcal{A}_{13} = \left(\frac{1}{2}\sigma^2+\alpha\sigma\Delta t\right)F_{0,\sigma} + \left(\frac{1}{2}\sigma^2+(\alpha-1)\sigma\Delta t-\left(\alpha-\frac{1}{2}\right)\Delta t^2\right)F_{1,\sigma} + \left(\frac{1}{2}\sigma^2+(\alpha-2)\sigma\Delta t-2(\alpha-1)\Delta t^2\right)F_{2,\sigma} \quad (58)$$

$$\mathcal{A}_{21} = F'_{0,\sigma} + F'_{1,\sigma} + F'_{2,\sigma} \quad (59)$$

$$\mathcal{A}_{22} = (\sigma+\alpha\Delta t)F'_{0,\sigma} + (\sigma+(\alpha-1)\Delta t)F'_{1,\sigma} + (\sigma+(\alpha-2)\Delta t)F'_{2,\sigma} \quad (60)$$

$$\mathcal{A}_{23} = \left(\frac{1}{2}\sigma^2+\alpha\Delta t\right)F'_{0,\sigma} + \left(\frac{1}{2}\sigma^2+(\alpha-1)\sigma\Delta t-\left(\alpha-\frac{1}{2}\right)\Delta t^2\right)F'_{1,\sigma} + \left(\frac{1}{2}\sigma^2+(\alpha-2)\sigma\Delta t-2(\alpha-1)\Delta t^2\right)F'_{2,\sigma} \quad (61)$$

$$\mathcal{A}_{31} = F''_{0,\sigma} + F''_{1,\sigma} + F''_{2,\sigma} \quad (62)$$

$$\mathcal{A}_{32} = (\sigma+\alpha\Delta t)F''_{0,\sigma} + (\sigma+(\alpha-1)\Delta t)F''_{1,\sigma} + (\sigma+(\alpha-2)\Delta t)F''_{2,\sigma} \quad (63)$$

$$\mathcal{A}_{33} = \left(\frac{1}{2}\sigma^2+\alpha\Delta t\right)F''_{0,\sigma} + \left(\frac{1}{2}\sigma^2+(\alpha-1)\sigma\Delta t-\left(\alpha-\frac{1}{2}\right)\Delta t^2\right)F''_{1,\sigma} + \left(\frac{1}{2}\sigma^2+(\alpha-2)\sigma\Delta t-2(\alpha-1)\Delta t^2\right)F''_{2,\sigma} \quad (64)$$

with the abbreviations

$$F_{0,\sigma} = F_0(-\sigma) \quad (65)$$

$$F_{1,\sigma} = F_1(\Delta t-\sigma) \quad (66)$$

$$F_{2,\sigma} = F_2(2\Delta t-\sigma). \quad (67)$$

To obtain a third order accurate interpolation scheme for $\hat{u}$, one needs $|\hat{u}(\tau_k)-u_\sigma| = \mathcal{O}(\Delta t^3)$, which is satisfied if $\mathcal{A}_{11} = 1$, $\mathcal{A}_{12} = 0$, and $\mathcal{A}_{13} = 0$. These three conditions can be rewritten into conditions on the temporal basis functions as

$$F_{0,\sigma} + F_{1,\sigma} + F_{2,\sigma} = 1 \quad (68)$$

$$F_{1,\sigma} + 2F_{2,\sigma} = \frac{\sigma}{\Delta t} + \alpha \quad (69)$$

$$F_{1,\sigma} + 4F_{2,\sigma} = \frac{\sigma^2}{\Delta t^2} + 2\alpha\frac{\sigma}{\Delta t} + 2\alpha^2. \quad (70)$$

It can be shown that conditions (68), (69) and (70) imply $\mathcal{A}_{21} = 0$, $\mathcal{A}_{22} = 1$, $\mathcal{A}_{23} = 0$, $\mathcal{A}_{31} = 0$, $\mathcal{A}_{32} = 0$, and $\mathcal{A}_{33} = 1$ for all $\sigma \in [0, \Delta t)$. Hence $|\hat{u}'(\tau_k)-u'_\sigma| = \mathcal{O}(\Delta t^2)$ and $|\hat{u}''(\tau_k)-u''_\sigma| = \mathcal{O}(\Delta t)$.

Concluding, if a temporal basis function satisfies conditions (68), (69) and (70), a first order accurate interpolation procedure has been obtained for the MOT scheme of the CFIE.

ACKNOWLEDGMENT

The authors would like to thank the anonymous reviewers for their helpful suggestions.

REFERENCES

[1] B. Shanker, A. A. Ergin, K. Aygün, and E. Michielssen, "Analysis of transient electromagnetic scattering phenomena using a two-level plane wave time-domain algorithm," *IEEE Trans. Antennas Propag.*, vol. 48, no. 4, pp. 510–523, 2000.

[2] A. E. Yilmaz, J.-M. Jin, E. Michielssen, and D. S. Weile, "A fast Fourier transform accelerated marching-on-in-time algorithm for electromagnetic analysis," *Electromagn.*, vol. 21, pp. 181–197, 2011.

[3] A. Sadigh and E. Arvas, "Treating the instabilities in marching-on-in-time method from a different perspective," *IEEE Trans. Antennas Propag.*, vol. 41, no. 12, pp. 1695–1702, 1993.

[4] S. J. Dodson, S. P. Walker, and M. J. Bluck, "Implicitness and stability of time domain integral equation scattering analyses," *ACES Journal*, vol. 13, pp. 291–301, 1998.

[5] Y. Shi, M.-Y. Xia, R.-S. Chen, E. Michielssen, and M. Lu, "Stable electric field TDIE solvers via quasi-exact evaluation of MOT matrix elements," *IEEE Trans. Antennas Propag.*, vol. 59, no. 2, pp. 574–585, 2011.

[6] D. S. Weile, G. Pisharody, N.-W. Chen, B. Shanker, and E. Michielssen, "A novel scheme for the solution of the time-domain integral equations of electromagnetics," *IEEE Trans. Antennas Propag.*, vol. 52, no. 1, pp. 283–295, 2004.

[7] F. P. Andriulli, K. Cools, F. Olyslager, and E. Michielssen, "Time domain Calderón identities and their application to the integral equation analysis of scattering by PEC objects Part II: Stability," *IEEE Trans. Antennas Propag.*, vol. 57, no. 8, pp. 2365–2375, 2009.

[8] T. Abboud, J.-C. Nédélec, and J. Volakis, "Stable solution of the retarded potential equations," in *Proc. ACES Conf.*, Monterey, CA, 2001, pp. 146–151.

[9] X. Wang, R. A. Wildman, D. S. Weile, and P. Monk, "A finite difference delay modeling approach to the discretization of the time domain integral equations of electromagnetics," *IEEE Trans. Antennas Propag.*, vol. 56, no. 8, pp. 2442–2452, 2008.

[10] S. M. Rao and D. R. Wilton, "Transient scattering by conducting surfaces of arbitrary shape," *IEEE Trans. Antennas Propag.*, vol. 39, pp. 56–61, 1991.

[11] G. Manara, A. Monorchio, and R. Reggiannini, "A space-time discretization criterion for a stable time-marching solution of the electric field integral equation," *IEEE Trans. Antennas Propag.*, vol. 45, no. 3, pp. 527–532, 1997.
[12] J.-L. Hu and C. H. Chan, "Improved temporal basis function for time domain electric field integral equation method," *Electron. Lett.*, vol. 35, no. 11, pp. 883–885, 1999.
[13] J.-L. Hu, C. H. Chan, and Y. Xu, "A new temporal basis function for the time-domain integral equation method," *IEEE Microw. Wireless Compon. Lett.*, vol. 11, no. 11, pp. 465–466, 2001.
[14] J.-L. Hu and C. H. Chan, "Novel approach to construct temporal basis functions for time-domain integral equation method," in *Proc. IEEE Int. Symp. Antennas Propag.*, Boston, MA, 2001, pp. 172–175.
[15] K. Aygün, B. Shanker, A. A. Ergin, and E. Michielssen, "A two-level plane wave time-domain algorithm for fast analysis of EMC/EMI problems," *IEEE Trans. Antennas Propag.*, vol. 44, no. 1, pp. 152–164, 2002.
[16] Y.-S. Chung, T. K. Sarkar, B. H. Jung, M. Salazar-Palma, Z. Ji, S. Jang, and K. Kim, "Solution of time domain electric field integral equation using the Laguerre polynomials," *IEEE Trans. Antennas Propag.*, vol. 52, no. 9, pp. 2319–2328, 2004.
[17] H. Bağci, A. E. Yilmaz, V. Lomakin, and E. Michielssen, "Fast solution of mixed-potential time-domain integral equations for half-space environments," *IEEE Trans. Geosci. Remote Sens.*, vol. 43, no. 2, pp. 269–279, 2005.
[18] Y. Shi and S. Li, "A solution of time domain integral equation using Hermite polynomials," in *Proc. IEEE Int. Symp. Microwave, Antenna, Propag. and EMC Techn. Wireless Comm.*, Hangzhou, 2007, pp. 864–867.
[19] G. X. Jiang, H. B. Zhu, G. Q. Ji, and W. Cao, "Improved stable scheme for the time domain integral equation method," *IEEE Microw. Wireless Compon. Lett.*, vol. 17, no. 1, pp. 1–3, 2007.
[20] P. Wang, M. Y. Xia, J. M. Jin, and L. Z. Zhou, "Time-domain integral equation solvers using quadratic B-spline temporal basis functions," *Microw. Opt. Technol. Lett.*, vol. 49, no. 5, pp. 1154–1159, 2007.
[21] A. Geranmayeh, W. Ackermann, and T. Weiland, "Temporal discretization choices for stable boundary element methods in electromagnetic scattering problems," *Appl. Numer. Math.*, vol. 59, pp. 2751–2773, 2009.
[22] M. H. Haddad, M. Ghaffari-Miab, and R. Faraji-Dana, "Transient analysis of thin-wire structures above a multilayer medium using complex-time green's functions," *IET Microw. Antennas Propag.*, vol. 4, no. 11, pp. 1937–1947, 2010.
[23] Z. H. Firouzeh, R. Moini, S. H. H. Sadeghi, R. Faraji-Dana, and G. A. E. Vandenbosch, "A new method for transient analysis of a dipole above a lossy ground using quadratic B-spline temporal basis functions," in *Proc. ICEAA*, Torino, 2011, pp. 982–985.
[24] Z. Mei, Y. Zhang, T. K. Sarkar, B. H. Jung, A. Garcia-Lamperez, and M. Salazar-Palma, "An improved marching-on-in-degree method using a new temporal basis," *IEEE Trans. Antennas Propag.*, vol. 59, no. 12, pp. 4643–4650, 2011.
[25] E. van 't Wout, H. van der Ven, D. R. van der Heul, and C. Vuik, "The accuracy of temporal basis functions used in the TDIE method," in *Proc. IEEE Int. Symp. Antennas Propag.*, Spokane, WA, 2011, pp. 2708–2711.
[26] B. Shanker, A. A. Ergin, K. Aygün, and E. Michielssen, "Analysis of transient electromagnetic scattering from closed surfaces using a combined field integral equation," *IEEE Trans. Antennas Propag.*, vol. 48, no. 7, pp. 1064–1074, 2000.
[27] S. M. Rao, D. R. Wilton, and A. W. Glisson, "Electromagnetic scattering by surfaces of arbitrary shape," *IEEE Trans. Antennas Propag.*, vol. 30, no. 3, pp. 409–418, 1982.
[28] B. H. Jung, Z. Ji, T. K. Sarkar, M. Salazar-Palma, and M. Yuan, "A comparison of marching-on in time method with marching-on in degree method for the TDIE solver," *PIER*, vol. 70, pp. 281–296, 2007.
[29] G. Kaur and A. E. Yilmaz, "Accuracy-efficiency tradeoff of temporal basis functions for time-marching solvers," *Microw. Opt. Technol. Lett.*, vol. 53, no. 6, pp. 1343–1348, 2011.
[30] B. Shanker, M. Lu, J. Yuan, and E. Michielssen, "Time domain integral equation analysis of scattering from composite bodies via exact evaluation of radiation fields," *IEEE Trans. Antennas Propag.*, vol. 57, no. 5, pp. 1506–1520, 2009.
[31] S. C. Brenner and L. R. Scott, *The Mathematical Theory of Finite Element Methods*, 3rd ed. New York: Springer, 2008.

Elwin van 't Wout was born in Rotterdam, Netherlands, in 1986. He received the M.S. degree in applied mathematics in 2009 from Delft University of Technology, where he is working towards the Ph.D. degree under the supervision of Prof. C. Vuik. The research for his master's thesis was carried out at the Maritime Research Institute Netherlands.

In 2009, he joined the National Aerospace Laboratory NLR, Amsterdam. His research focuses on time domain integral equation methods.

Duncan R. van der Heul was born in Rotterdam, Netherlands, in 1973. He received the M.S. degree in marine technology and the Ph.D. degree in applied mathematics, under the supervision of Prof. Wesseling, from Delft University of Technology, in 1997 and 2002, respectively.

From 2001 to 2008, he worked as a Research Engineer at the National Aerospace Laboratory NLR, Amsterdam. In 2008, he joined the Numerical Analysis Group of Prof. Vuik at Delft University of Technology as an Assistant Professor, where he focuses his research on computational fluid dynamics and computational electromagnetics.

Harmen van der Ven received the M.S. degree in mathematics and the Ph.D. degree from Utrecht University in 1989 and 1993, respectively.

Afterwards, he joined the Netherlands National Aerospace Laboratory, Amsterdam, where he now holds the position of Senior Scientist. His research interest is computational science, with applications in electromagnetics, fluid dynamics and mechanical engineering. In the field of electromagnetics the main focus is on the prediction of radar cross sections of large objects with radar absorbing treatment.

Cornelis Vuik received the M.S. degree in applied mathematics from Delft University of Technology in 1982. After a short stay at Philips Research Laboratories, he received the Ph.D. degree in mathematics from Utrecht University in 1988.

Thereafter, he became employed at the Delft University of Technology, where he holds the position of Full Professor of the Numerical Analysis Research Group. In 2007, he also became Director of the Delft Center of Computational Science and Engineering.